Band alignment modulation of atomic layer deposition-prepared Al2O3/ -Ga2O3 heterojunction interface by deposition temperature

Zhou, Shun; Liu, Hao; Dong, Linpeng; Song, Shigeng; Liu, Wenjun

Published in:
Journal of Vacuum Science and Technology A: Vacuum, Surfaces and Films

DOI:
10.1116/6.0000951

Published: 29/03/2021

Document Version
Peer reviewed version

Band alignment modulation of ALD-prepared Al_2O_3/β-Ga_2O_3 heterojunction interface by deposition temperature

Shun Zhou[1, a)], Hao Liu[2], Linpeng Dong[1], Weiguo Liu[1], Shigeng Song[3], Wenjun Liu[2, b)]

[1]School of Optoelectronic Engineering, Xi'an Technological University, Xi'an 710021, China

[2]State Key Laboratory of ASIC and System, School of Microelectronics, Fudan University, Shanghai 200433, China

[3]Institute of Thin Films, Sensors and Imaging, SUPA (Scottish Universities Physics Alliance), University of the West of Scotland, Scotland PA1 2BE, UK

[a)]Electronic mail: zhoushun@xatu.edu.cn

[b)]Electronic mail: wjliu@fudan.edu.cn

The band alignment between oxygen plasma-assisted atomic layer deposition (ALD) Al_2O_3 films and β-Ga_2O_3 (-201) substrates under different deposition temperatures was characterized by X-ray photoelectron spectroscopy (XPS). As the deposition temperature increased from 30 to 200 °C, all the heterojunctions exhibited a type-I alignment. The bandgap of Al_2O_3 enlarged from 6.26 ± 0.1 to 6.81 ± 0.1 eV, leading to the conduction band offset (CBO) varying linearly from 1.39 ± 0.1 to 1.95 ± 0.1 eV, while the valence band offset (VBO) was insensitive. This difference was attributed to Al ion deficiency and hydroxyl groups induced by the inadequate reaction of trimethylaluminium (TMA) under low deposition temperatures, which was proved by secondary ion mass spectrometry (SIMS) and Fourier-transform infrared spectroscopy (FTIR). These finding could facilitate the design of the CBO-controllable Al_2O_3/β-

Ga_2O_3 heterojunction through deposition temperature.

I. INTRODUCTION

β-Ga_2O_3 is one of the emerging wide-gap semiconductors for next-generation high-power electronic applications, which has gained extensive attention in recent years.[1-3] The theoretical maximal breakdown field of β-Ga_2O_3 is expected to be ~ 8MV/cm due to its ultrawide bandgap (4.6-4.9 eV),[4] and the Baliga's figure of merit ($\varepsilon\mu E_{br}^3$) is as high as 3444,[5] which exceeds the value of GaN and SiC.[6] Besides these excellent material properties, its mass production of high-quality single crystal β-Ga_2O_3 can be acquired by low-cost melt growth methods such as edge-defined film-fed (EDFG) and floating-zone (FZ) for commercial utilization.[7,8]

Over the past years, high-power metal-insulator semiconductor field-effect transistors (MISFETs) based on β-Ga_2O_3 have been demonstrated.[9,10] For practical MISFETs, the choice of gate insulator layer-plays an important role in obtaining high-performance transistors, the leakage current and on/off current ratio are mainly determined by the semiconductor/gate insulator interface. Up to now, several insulators including SiO_2,[11] Al_2O_3,[12] AlN,[13,14] *etc*. have been successively investigated for applications of β-Ga_2O_3 based FETs. Among which, Al_2O_3 is implemented extensively because of its moderately large bandgap (6.4-6.9 eV) and high dielectric constant of ~9. To evaluate the anti-leakage current stability of the gate insulator, the band alignment analysis of the gate insulator/β-Ga_2O_3 is necessary to calculate the VBO and CBO

across the gate insulator/bulk material.

Kamimura *et al.* investigated the band offset of ALD prepared Al_2O_3/β-Ga_2O_3 heterojunction using X-ray photoelectron spectroscopy (XPS),[12] and a bandgap for Al_2O_3 of 6.8 ± 0.2 eV was observed. Meanwhile, the VBO and CBO were calculated to be 0.7 ± 0.2 and 1.5 ± 0.2 eV, respectively. Carey *et al.* compared the influence of different deposition methods on the band alignment of Al_2O_3/β-Ga_2O_3 heterojunctions between radio-frequency (RF) magnetron sputtering and ALD methods.[15] The bandgaps of Al_2O_3 fabricated by the two methods were both 6.9 eV, while the CBO of 3.16 eV (2.23 eV) and the VBO of -0.86 eV (-0.07 eV) were measured for sputtering (ALD) method, respectively. Hung *et al.* quantitatively investigated the CBO and effects of interface fixed charges on ALD prepared Al_2O_3/β-Ga_2O_3 heterojunctions,[16] where a CBO of 1.7 eV was obtained. Thus, it can be concluded that the VBO and CBO of Al_2O_3/β-Ga_2O_3 heterojunctions are influenced by the preparation method and processing parameter, as well as the deposition temperature. However, a systematic investigation concerning the band alignment-temperature dependence of Al_2O_3/β-Ga_2O_3 heterojunction is absent so far. Furthermore, a tunable band alignment is desired for the degree of design freedom to meet specific demands. For instance, alloying processes such as $(Al_xGa_{1-x})_2O_3$ and $Hf_xAl_{1-x}O$ were adopted to characterize the VBO and CBO modulations of β-Ga_2O_3-based heterojunctions.[17,18] However, this method is limited by its complex procedure, and the prepared alloys are often subjected to the bowing behavior.[16,17]

Herein, this work presents the temperature-dependent band alignment of Al_2O_3/β-

Ga_2O_3 heterojunction, in which the Al_2O_3 films were prepared by an oxygen plasma-assisted ALD method. The band alignment and band offset values were characterized and determined. At last, the difference in the temperature dependence of VBO and CBO was further discussed and proved by SIMS and FTIR.

II. EXPERIMENTAL

All Al_2O_3 films in this study were deposited using ALD with trimethylaluminum (TMA, purity: 99.999%, Fornano, Suzhou, China) and O_2 plasma as Al and O precursors, respectively. Prior to the Al_2O_3 deposition, β-Ga_2O_3 substrates were cleaned in solvent (acetone/isopropanol/deionized water) to remove the residual contaminations, and then were loaded into ALD reactor (Picosun R-200 Advanced, Finland) for Al_2O_3 deposition. One growth cycle consisted of 0.1 s TMA pulse, 10 s N_2 purge, 8 s O_2 plasma pulse, and 10 s N_2 purge. The TMA was maintained at 18 ºC for a stable vapor pressure and dose, and the O_2 gas flow rate was fixed at 150 sccm using a remote plasma generator (Advanced energy, USA) with the power of 2500 W. The reaction chamber pressure was kept at ~1000 Pa. Three types of samples were prepared for XPS measurements: (1) bulk (-201) β-Ga_2O_3 substrates (Sn-doping, 4.2×10^{18} cm^{-3}) grown by floating-zone method, (2) 40 nm-thick Al_2O_3 films deposited on β-Ga_2O_3 substrates under 30, 50, 100, 150 and 200 °C, respectively, and (3) 3nm-thick Al_2O_3 films deposited on β-Ga_2O_3 substrates under 30, 50, 100, 150 and 200 °C, respectively. The XPS measurements were carried out by using a monochromatic Al Kα1 X-radiation source (1486.7 eV). All high-resolution binding energy spectra were collected in a step

of 0.05 eV. The C 1*s* peak located at 284.8 eV was adopted as the calibration reference. Reflection electron energy loss spectroscopy (REELS) was used to determine the bandgap E_g of the deposited films. Secondary ion mass spectrometry (SIMS) (PHI Adept 1010, Japan) with Cs primary ion beam with an energy of 3 keV was employed for profiling Ga, Al, and H elements concentration distributions. The Fourier-transform infrared spectroscopy (FTIR) ranged from 4000-1000 cm^{-1} with a resolution of 2 cm^{-1} was performed using a TENSOR II Bruker spectrometer at room temperature.

III. RESULTS AND DISCUSSION

Figure 1 shows the O 1*s* core-level REELS spectra of 40 nm-thick Al_2O_3 films deposited under different temperatures, the bandgap E_g of the deposited Al_2O_3 film was defined as the intercept energy between flat and linear slope regions. As the deposition temperature increases, the linear slope region shifts to a higher loss energy, leading to the enlargement of the bandgap. For the sample deposited under 30 °C, the extracted E_g is 6.26 ± 0.1 eV, and the E_g rises to 6.81 ± 0.1 eV as the deposition temperature increased to 200 °C. Detailed E_g under different deposition temperatures were listed in Table 1.

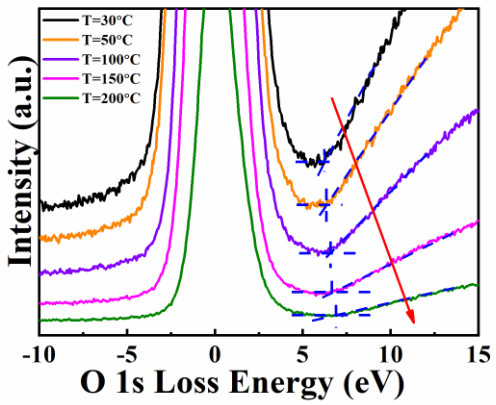

FIG. 1. O 1*s* core-level REELS spectra of 40 nm-thick Al_2O_3 films deposited on β-Ga_2O_3 substrate under different deposition temperatures.

To investigate the band alignment of the Al_2O_3/β-Ga_2O_3 heterojunction, high-resolution XPS was utilized to record the core-level spectra, and the VBM position of Al_2O_3 and β-Ga_2O_3 were estimated through a linear extrapolation of the leading edge to the baseline of the valence band spectra. According to Kraut's theory, the VBO (ΔE_V) can be calculated by the following formula[19]

$$\Delta E_V = \left(E_{Ga3d}^{Ga_2O_3} - E_{VBM}^{Ga_2O_3}\right) - \left(E_{Al2p}^{Al_2O_3} - E_{VBM}^{Al_2O_3}\right) + \left(E_{Ga3d}^{Heterojunction} - E_{Al2p}^{Heterojunction}\right) \quad (1)$$

where $E_{Ga3d}^{Ga_2O_3}$ and $E_{VBM}^{Ga_2O_3}$ corresponds to the peak positions of the Ga 3d core level and VBM for bulk β-Ga_2O_3, respectively. $E_{Al2p}^{Al_2O_3}$ and $E_{VBM}^{Al_2O_3}$ are the peak positions of the Al 2p core level and VBM for 40 nm-thick Al_2O_3 film, respectively. $E_{Ga3d}^{Heterojunction}$ and $E_{Al2p}^{Heterojunction}$ represent the peak positions of the Ga 3*d* and Al 2*p* core levels in the heterojunction, respectively.

Figure 2(a) and 2(b) present the binding energy differences for 40 nm-thick Al_2O_3 film (Al 2*p*) and bulk β-Ga_2O_3 (Ga 3*d*), respectively. The VBM positions for Al_2O_3 and β-Ga_2O_3 are 3.47 and 3.53 eV, respectively. The core levels for Al 2*p* and Ga 3*d* are located at 74.48 (Al-O bond) and 20.37 eV (Ga-O bond), respectively, consistent with previous reports.[13,15,16] From Eq. (2), the VBO of the Al_2O_3/β-Ga_2O_3 heterojunction deposited under 30 °C was calculated to be 0.22 ± 0.05 eV. Based on the obtained VBO, the CBO (ΔE_C) was subsequently calculated by

$$\Delta E_C = E_g^{Al_2O_3} - E_g^{Ga_2O_3} - \Delta E_V \quad (2)$$

where $E_g^{Al_2O_3}$ and $E_g^{Ga_2O_3}$ are the bandgap of Al_2O_3 and β-Ga_2O_3, respectively. According our previous report, the estimated $E_g^{Ga_2O_3}$ was 4.65 ± 0.1 eV,[20] which was extracted from O 1*s* core-level REELS spectrum. Based on the aforemention, the CBO was calculated to be 1.39 ± 0.1 eV. Similarly, the VBOs and CBOs for Al_2O_3/β-Ga_2O_3 heterojunctions deposited under higher temperatures were evaluated, as shown in Table 1.

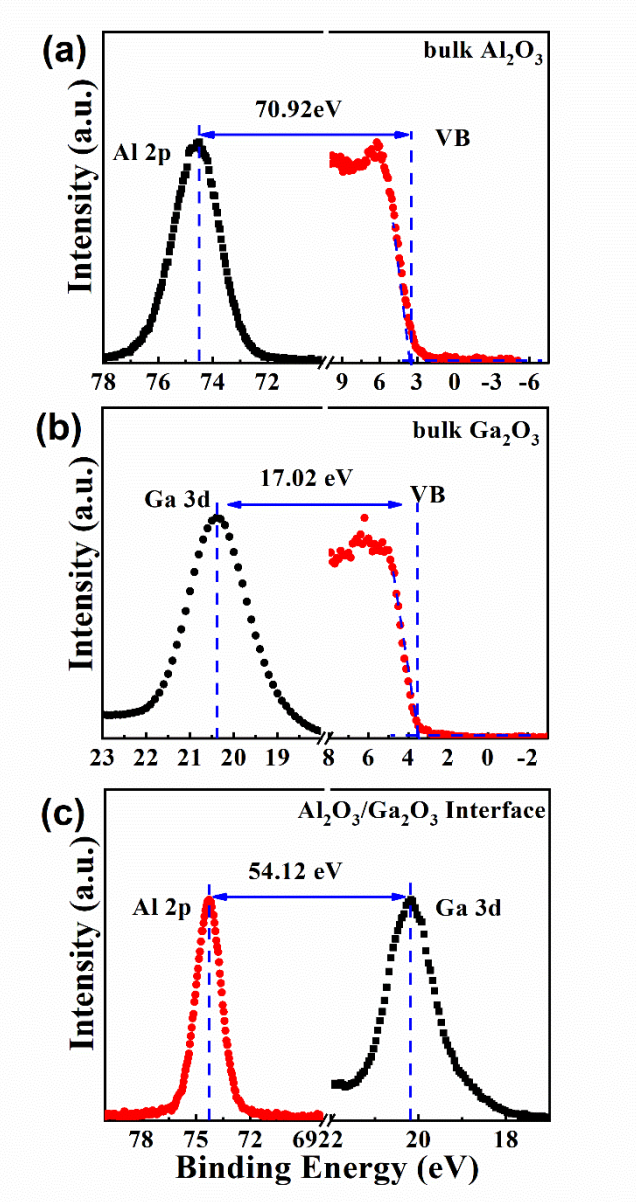

FIG. 2. Binding energy differences of (a) Al 2*p* and VBM for bulk Al_2O_3, (b) Ga 3*d* and VBM for bulk β-Ga_2O_3, and (c) Al 2*p* and Ga 3*d* for the Al_2O_3/β-Ga_2O_3 heterojunction deposited at 30 °C.

TABLE I. The bandgaps of Al_2O_3 films, the VBOs and CBOs for Al_2O_3/β-Ga_2O_3 heterojunctions, and the O/Al atoms ratio in Al_2O_3 films deposited under different temperatures. The standard deviations for bandgap, VBO, and EBO ration are ± 0.1, ± 0.05, and ± 0.1 eV, respectively.

Temperature (°C)	Al_2O_3 bandgap (eV)	VBO (eV)	EBO (eV)	O/Al atoms ratio
30	6.26	0.22	1.39	1.97
50	6.35	0.21	1.49	1.96
100	6.60	0.21	1.74	1.75
150	6.71	0.20	1.86	1.61
200	6.81	0.21	1.95	1.40

The detailed energy band alignment of Al_2O_3/*β*-Ga_2O_3 heterojunctions deposited under different temperatures was plotted, as shown in Figure 3. All the band alignments exhibit a typical straddled (type-I) feature. With deposition temperature rising from 30 to 200 °C, the bandgap of Al_2O_3 increases from 6.26 ± 0.1 to 6.81 ± 0.1 eV, and the CBO of Al_2O_3/*β*-Ga_2O_3 heterojunction increases from 1.39 ± 0.1 to 1.95 ± 0.1 eV by 0.56 eV. While the VBO is insensitive to the Al_2O_3 film deposition temperature and keeps around 0.21 ± 0.05 eV.

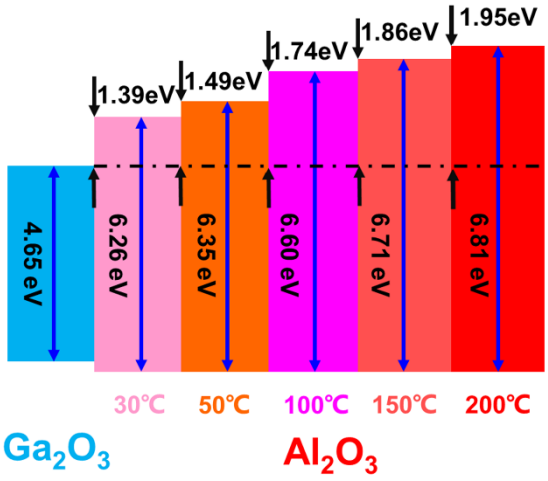

FIG. 3. The band alignment of Al_2O_3/β-Ga_2O_3 heterojunctions under different deposition temperatures.

The CBOs and VBOs of Al_2O_3/β-Ga_2O_3 heterojunction as a function of deposition temperature was plotted in Figure. 4(a). The CBO exhibits a ~50 times higher linear deposition-temperature dependence (the slope coefficient is 0.00333) than VBO (the slope coefficient is -0.000006). This implies that the CBO for the Al_2O_3/β-Ga_2O_3 system can be linearly modulated by the ALD temperature, which is more controllable and easier than alloying method such as $(Al_xGa_{1-x})_2O_3$ and $Hf_xAl_{1-x}O$.[17,18]

To figure out this CBO linear deposition-temperature dependence, the Al/O atoms ratio and bandgap value for 40 nm-thick Al_2O_3 film as a function of deposition temperature were also presented, as shown in Figure 4(b). The O/Al atoms ratio decreases linearly with the deposition temperature, the O/Al atoms ratio for 40 nm-thick Al_2O_3 film prepared under 30 and 200 °C are 1.97 and 1.40, respectively. While the bandgap of Al_2O_3 film enlarges linearly with the deposition temperature. These results indicate that the VBM position is insensitive to the deposition temperature, while

the increased deposition temperature leads to the O/Al atoms ratio decreases to meet the ideal stoichiometry of Al_2O_3 (3:2). The enlarged bandgap further shifts the CBM of Al_2O_3 to a higher energy, resulting in an increased CBO which is sensitive to the deposition temperature.

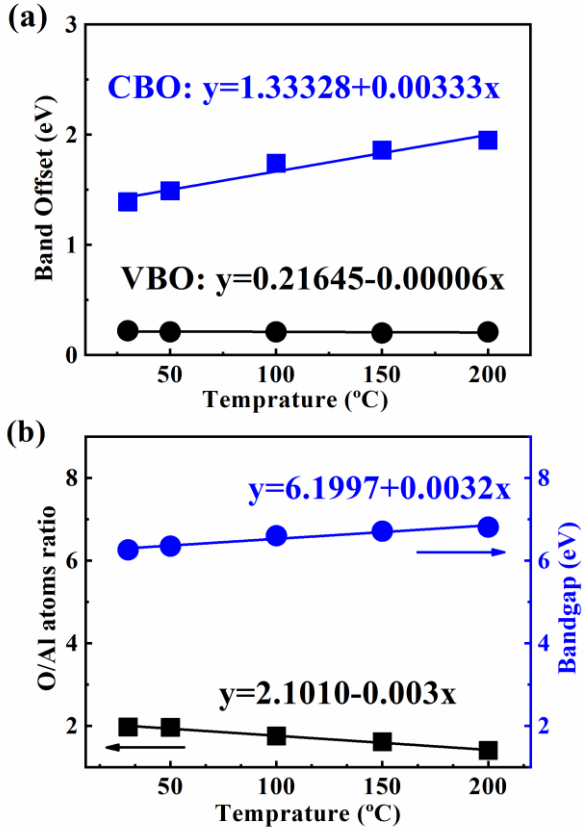

FIG. 4. Temperature dependence of (a) CBO and VBO, (b) bandgap and O/Al ratio of Al_2O_3 in the range of 30 - 200 °C.

Next, SIMS was utilized to examine the H concentration distribution in the Al_2O_3 films, the result is shown in Figure 5. The H concentration in the Al_2O_3 film grown under 200 °C is ~2.92×10^{21} atoms/cc, which is obviously lower than the value for the sample deposited at 30 °C (~6.88×10^{21} atoms/cc). The inset of Figure 5 displays the Al, Ga, and H elements distributions in Al_2O_3/β-Ga_2O_3 heterojunction, the abrupt

variations of the Al and Ga elements indicate the high-quality interface between Al_2O_3 and β-Ga_2O_3 substrate. To further track the excessive O and H elements in Al_2O_3 films, FTIR spectra were adopted to analyze the components. Figure 6 shows the FTIR spectra of Al_2O_3 films grown by ALD under temperatures of 30 and 200 °C. Obviously, a few peaks around 1600 cm^{-1} which are assigned to C-H, C=O, and C=C stretching vibration emerge in the Al_2O_3 deposited under 30 °C,[21,22] while the peak at 3750 cm^{-1} is related to hydroxyl group (-OH).[23] In contrast, the Al_2O_3 film deposited at 200 °C exhibits weak peaks around both 3750 cm^{-1} and 1600 cm^{-1}. These results imply that there are more C-H, C=O, and C=C bonds, accompanied with hydroxyl groups in the Al_2O_3 film under low deposition temperature. It can be attributed to the inadequate reaction between TMA and O_2 plasma. These FTIR spectra features are also in good agreement with SIMS results.

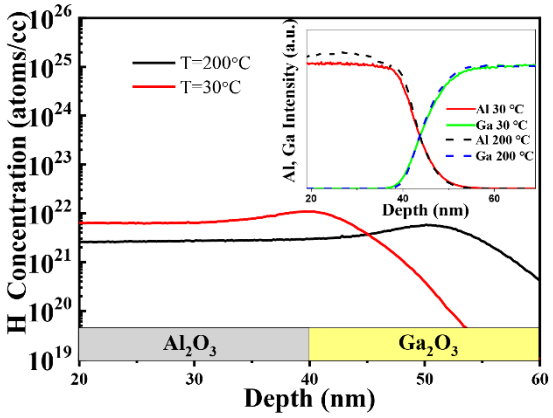

FIG. 5. H concentration in Al_2O_3 films grown under deposition temperatures of 30 °C and 200 °C derived from SIMS measurements. The inset plots H, Al, Ga concentrations with different depths at 30 °C.

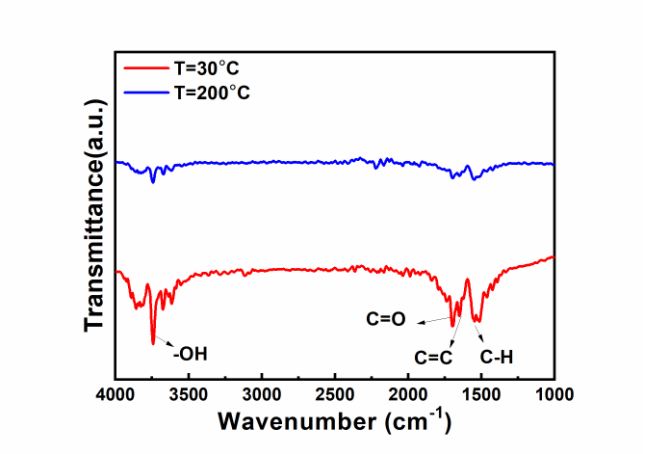

FIG. 6. FTIR spectra of Al_2O_3 films grown by ALD under deposition temperatures of 30 and 200 °C.

Previous studies revealed that under low-deposition temperature (below the crystallization temperature),[24,25] the Al_2O_3 film density increases with the deposition temperature. For Al_2O_3 film deposited under 30 °C, the lower film density and high O/Al atoms ratio (exceeds 3:2) indicate the film is loosened with high-density vacancies and cavities. In our deposition process, the O_2 plasma with high energy makes the film fully oxidized, while the low deposition temperature leads to the inadequate reaction of TMA. The dissociative Al ions and hydroxy groups induced by the un-reacted TMA can fill the vacancies and cavities in the films, which were deposited under low temperatures. First-principles calculations results indicated both the VBMs of Al_2O_3 and Ga_2O_3 are derived from O 2*p* orbitals,[26,27] while the VBMs for Al_2O_3 and Ga_2O_3 mainly consist of Al 3*s* and Ga 4*s* orbitals, respectively. The deficiency of Al ions as well as hydroxy groups and vacancies dominate the CBM position,[28,29] making the CBO sensitive to the deposition temperature. As the deposition temperature increases to 200 °C, the dense Al_2O_3 film with ideal elemental chemical ratio restrains the vacancies

and cavities appearance, then the Al_2O_3 bandgap is enlarged. While the adequate O ions from O_2 plasma ensure the VBM of Al_2O_3 pinned at a specific energy, thus the VBO is immune to the deposition temperature.

IV. SUMMARY AND CONCLUSIONS

In summary, we have investigated the band alignment modulation of ALD-prepared Al_2O_3/β-Ga_2O_3 heterojunction. As the deposition temperature increased from 30 to 200 °C, all the heterojunctions exhibited type-I alignment characteristic. The bandgap of Al_2O_3 enlarged from 6.26 ± 0.1 to 6.81 ± 0.1 eV, leading the conduction band offset (CBO) varying linearly from 1.39 ± 0.1 to 1.95 ± 0.1 eV, while the valence band offset (VBO) was insensitive. This difference was attributed to the Al ions deficiency and hydroxyl groups induced by the inadequate reaction of TMA under low deposition temperatures. These finding could facilitate the design of the CBO-controllable Al_2O_3/β-Ga_2O_3 heterojunction through deposition temperature.

ACKNOWLEDGMENTS

The authors would like to acknowledge the financial support partially by the Advanced Optical Manufacturing and Detection Innovation Team project of Shaanxi Provincial Science and Technology Department (2017KCT-08-02), the Key-Area Research and Development Program of Guangdong Province (2019B010128001), National Natural Science Foundation of China (61774041), and Shanghai Science and Technology Innovation Program (Grant No.19520711500).

DATA AVAILABILITY

The data that support the findings of this study are available from the corresponding author upon reasonable request.

REFERENCES

[1]H. H. Tippins, Phys. Rev. **140**, A316 (1965).

[2]M. Orita, H. Ohta, M. Hirano, and H. Hosono, Appl. Phys. Lett. **77**, 4166 (2000).

[3]M. Higashiwaki, K. Sasaki, and H. Murakami, Semicond. Sci. Tech. **31**, 034001 (2016).

[4]S. J. Pearton, Jiancheng Yang, Patrick H Cary IV, F Ren, Jihyun Kim, Marko J Tadjer, and Michael A. Mastro, Appl. Phys. Rev. **5**, 011301 (2018).

[5]B. J. Baliga, IEEE Electr. Device Lett. **10**, 455 (1989).

[6]M. Higashiwaki, K. Sasaki, A. Kuramata, T. Masui, and S. Yamakoshi, Appl. Phys. Lett. **100,** 013504 (2012).

[7]Akito Kuramata, Kimiyoshi Koshi, Shinya Watanabe, Yu Yamaoka, Takekazu Masui, and Shigenobu Yamakoshi, Jpn. J. Appl. Phys. **55**, 1202A2 (2016).

[8]Encarnación G Víllora, Kiyoshi Shimamura, Yukio Yoshikawa, Kazuo Aoki, and Noboru Ichinose, J. Cryst. Growth **270**, 420 (2004).

[9]Zongyang Hu, Kazuki Nomoto, Wenshen Li, Nicholas Tanen, Kohei Sasaki, Akito Kuramata, Tohru Nakamura, Debdeep Jena, and Huili Grace Xing, IEEE Electr. Device Lett. **39**, 869 (2018).

[10]Kosuke Matsuzaki, Hidenori Hiramatsu, Kenji Nomura, Hiroshi Yanagi, Toshio Kamiya, Masahiro Hirano, and Hideo Hosono, Thin Solid Films **496**, 37 (2006).

[11]Ye Jia, Ke Zeng, Joshua S Wallace, Joseph A Gardella, and Uttam Singisetti, Appl. Phys. Lett. **106**, 102107 (2015).

[12]Takafumi Kamimura, Kohei Sasaki, Man Hoi Wong, Daivasigamani Krishnamurthy, Akito Kuramata, Takekazu Masui, Shigenobu Yamakoshi, and Masataka Higashiwaki, Appl. Phys. Lett. **104**, 192104 (2014).

[13]Haiding Sun, CG Torres Castanedo, Kaikai Liu, Kuang-Hui Li, Wenzhe Guo, Ronghui Lin, Xinwei Liu, Jingtao Li, and Xiaohang Li, Appl. Phys. Lett. **111**, 162105 (2017).

[14]Jin-Xin Chen, Jia-Jia Tao, Hong-Ping Ma, Hao Zhang, Ji-Jun Feng, Wen-Jun Liu, Changtai Xia, Hong-Liang Lu, and David Wei Zhang, Appl. Phys. Lett. **112**, 261602 (2018).

[15]Patrick H Carey IV, F Ren, David C Hays, BP Gila, SJ Pearton, Soohwan Jang, and Akito Kuramata, Vacuum, **142**, 52 (2017).

[16]Ting-Hsiang Hung, Kohei Sasaki, Akito Kuramata, Digbijoy N Nath, Pil Sung Park, Craig Polchinski, and Siddharth Rajan, Appl. Phys. Lett. **104**, 162106 (2014).

[17]Ryo Wakabayashi, Mai Hattori, Kohei Yoshimatsu, Koji Horiba, Hiroshi Kumigashira, and Akira Ohtomo, Appl. Phys. Lett. **112**, 232103 (2018).

[18]Hongpeng Zhang, Lei Yuan, Renxu Jia, Xiaoyan Tang, Jichao Hu, Yimen Zhang, Yuming Zhang, and Jianwu Sun, J. Phys. D Appl. Phys. **52**, 215104 (2019).

[19]EA Kraut, RW Grant, JR Waldrop, and SP Kowalczyk, Phys. Rev. Lett. **44**, 1620 (1980).

[20]Shun-Ming Sun, Wen-Jun Liu, Yong-Ping Wang, Ya-Wei Huan, Qian Ma, Bao Zhu, Su-Dong Wu, Wen-Jie Yu, Ray-Hua Horng, and Chang-Tai Xia, Appl. Phys. Lett. **113**, 031603 (2018).

[21]Rino Morent, Nathalie De Geyter, Christophe Leys, L Gengembre, E Payen, Surf. Interface Anal. **40**, 597 (2008).

[22]Bo Gong and Gregory N Parsons, J. Mater. Chem. **22,** 15672 (2012).

[23]Peter R Solomon and Robert M Carangelo, Fuel **61**, 663 (1982).

[24]G Dingemans, M. C. M. Van de Sanden, W. M. M. Kessels, Electrochem. ECS Solid State Lett. **13**, H76 (2009).

[25]MD Groner, FH Fabreguette, JW Elam, and SM George, Chem. Mater. **16**, 639 (2004).

[26]Shun-Li Shang, Hui Zhang, Yi Wang, and Zi-Kui Liu, J. Phys-Condens. Mat. **22**, 375403 (2010).

[27]Haiying He, Roberto Orlando, Miguel A Blanco, Ravindra Pandey, Emilie Amzallag, Isabelle Baraille, and Michel Rérat, Phys. Rev. B **74**, 195123 (2006).

[28]D Liu, Y Guo, L Lin, and J Robertson, J. Appl. Phys. **114**, 083704 (2013).

[29]Katsuyuki Matsunaga, Tomohito Tanaka, Takahisa Yamamoto, and Yuichi Ikuhara, Phys. Rev. B **68**, 085110 (2003).